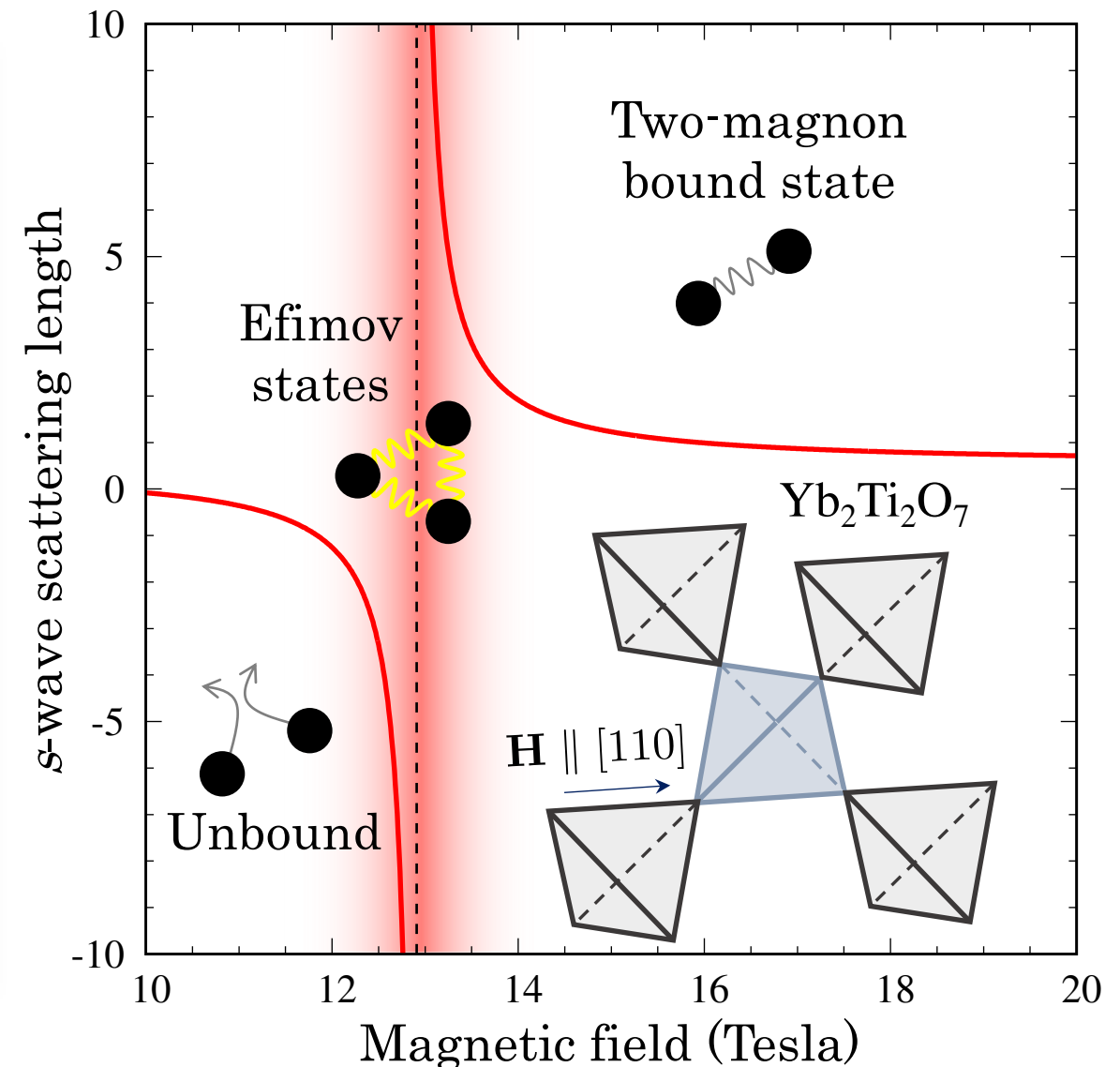


Magnetic-field-induced tunability of magnon bound states: Scattering resonances and Efimov states in $\text{Yb}_2\text{Ti}_2\text{O}_7$

Key takeaways:

- The scattering length between magnons is tunable by a uniform magnetic field. (Counterpart of Feshbach resonance in ultracold atomic gases)
- Efimov bound states are expected in the vicinity of the unitarity limit.



Yasuyuki Kato, U. Tokyo

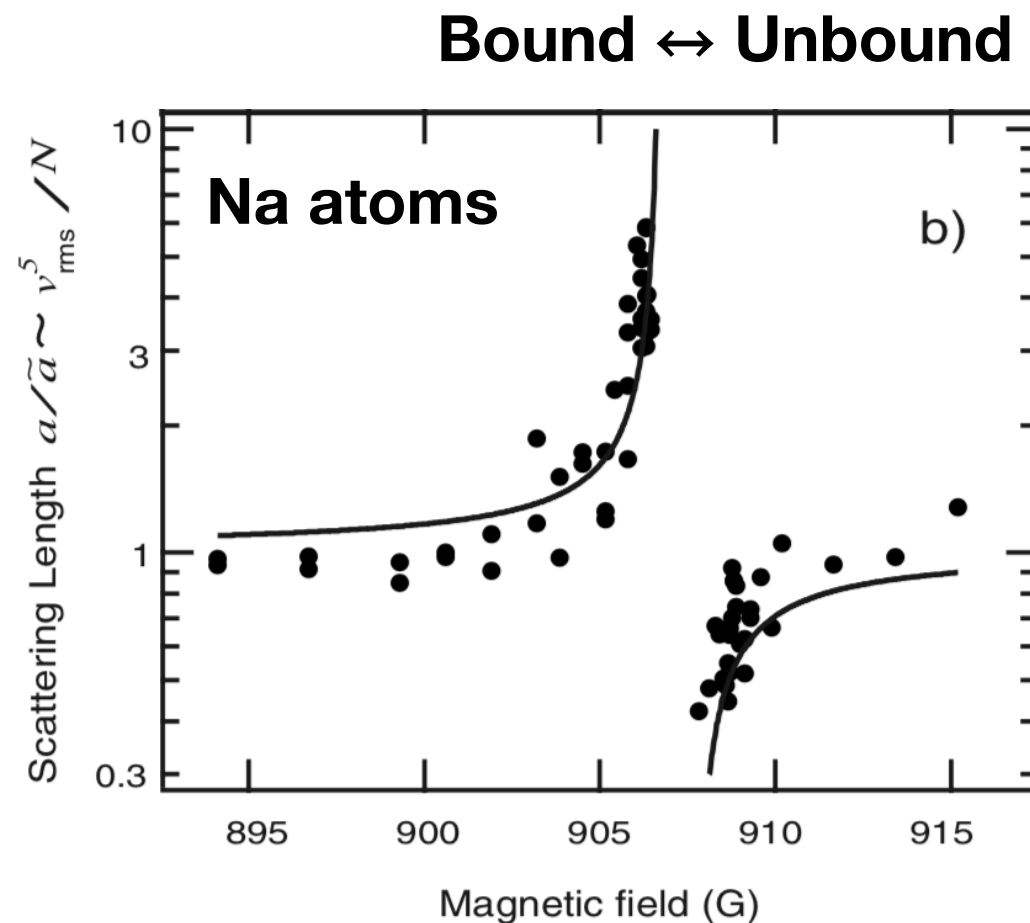
Collaborators: Shang-Shun Zhang^A, Yusuke Nishida^B, C. D. Batista^{A,C}
^AU. Tennessee, ^BTokyo Tech, ^CORNL

Publication: Phys. Rev. Research **2**, 033024 (2020).

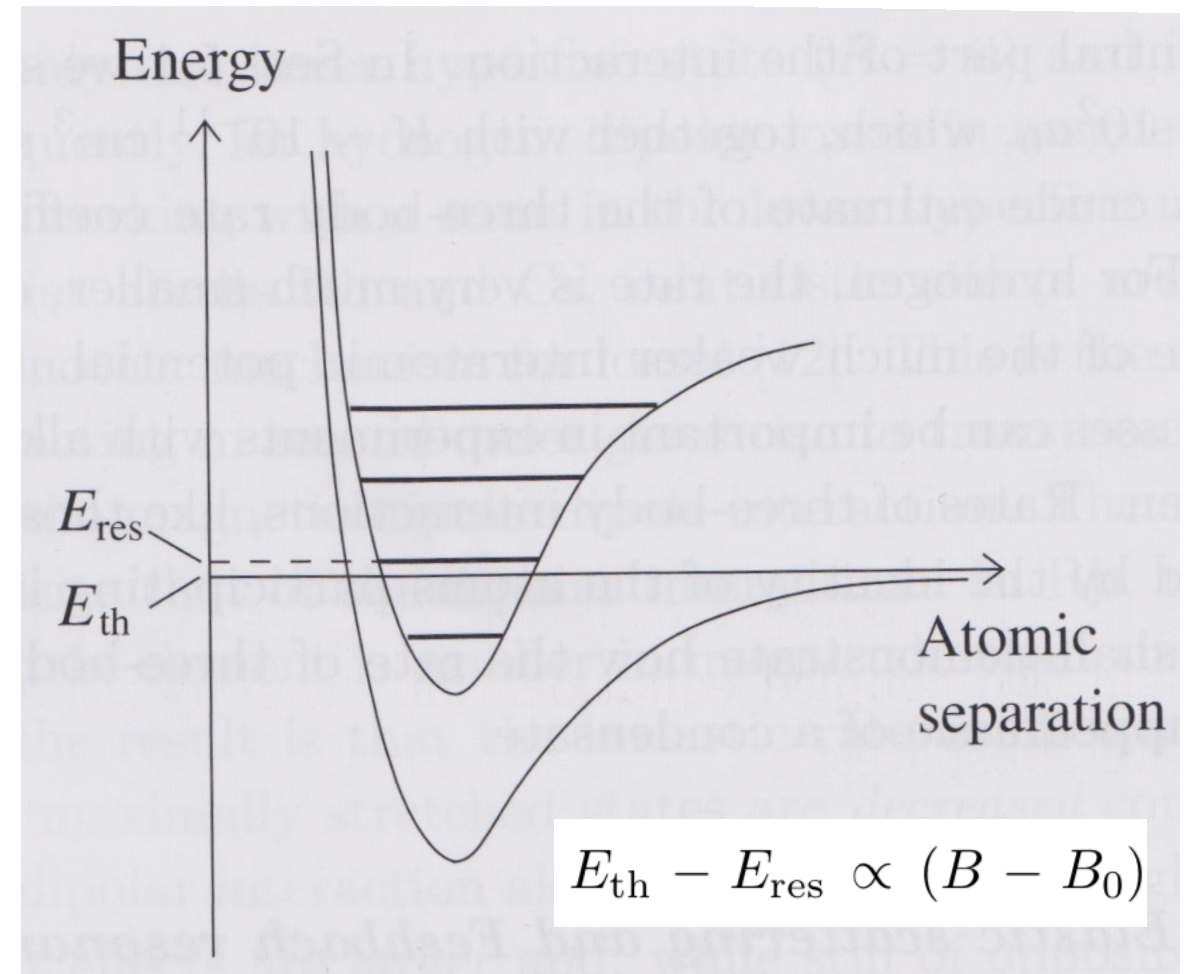
2021/03/25

Feshbach resonance in ultracold atomic gases

Review article: C. Chin *et al.*, RMP 2010.



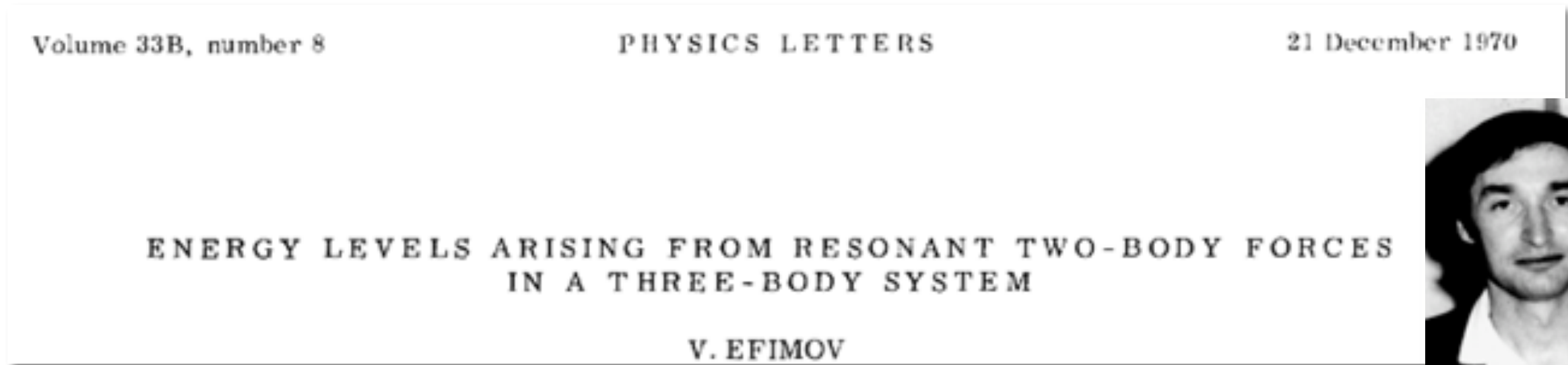
S. Inouye *et al.*, PRL (2004)



C. J. Pethick & H. Smith, "Bose-Einstein Condensation in Dilute Gases (2nd Ed)", Cambridge Univ. Press (2008).

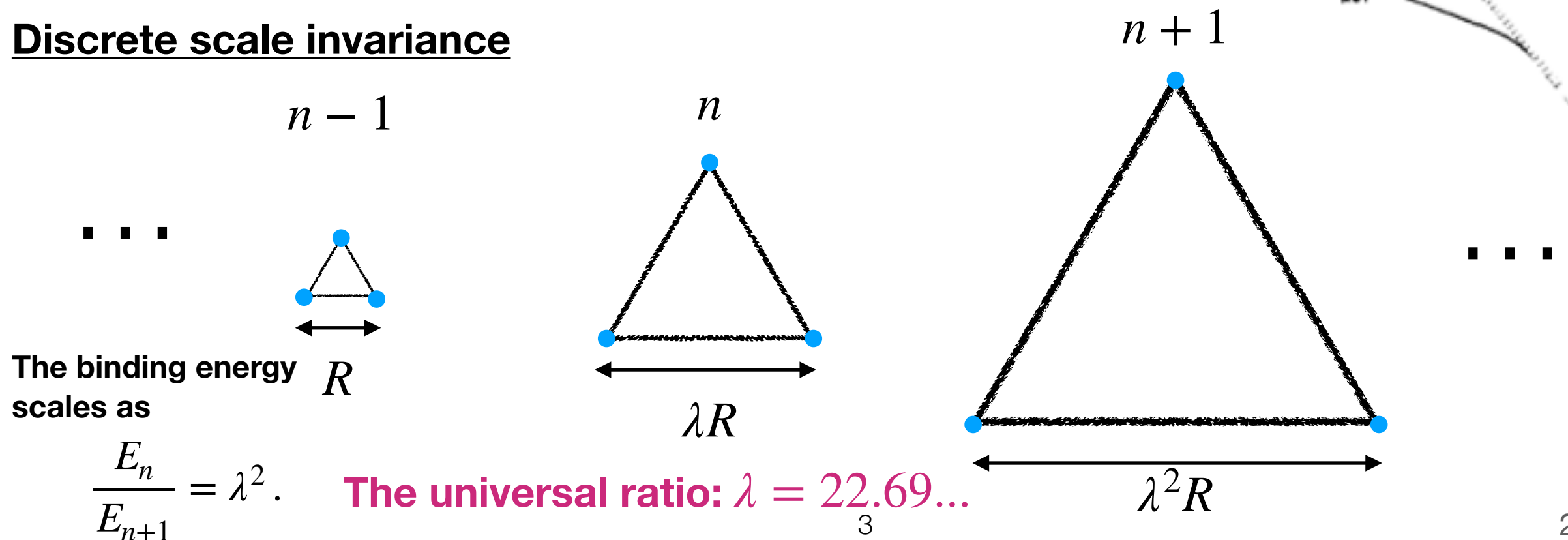
The s-wave scattering length a can be varied by applying a uniform magnetic field.
→ Efimov bound states are found in ultracold atomic gases [T. Kraemer *et al.*, Nature (2006)].

Efimov effect



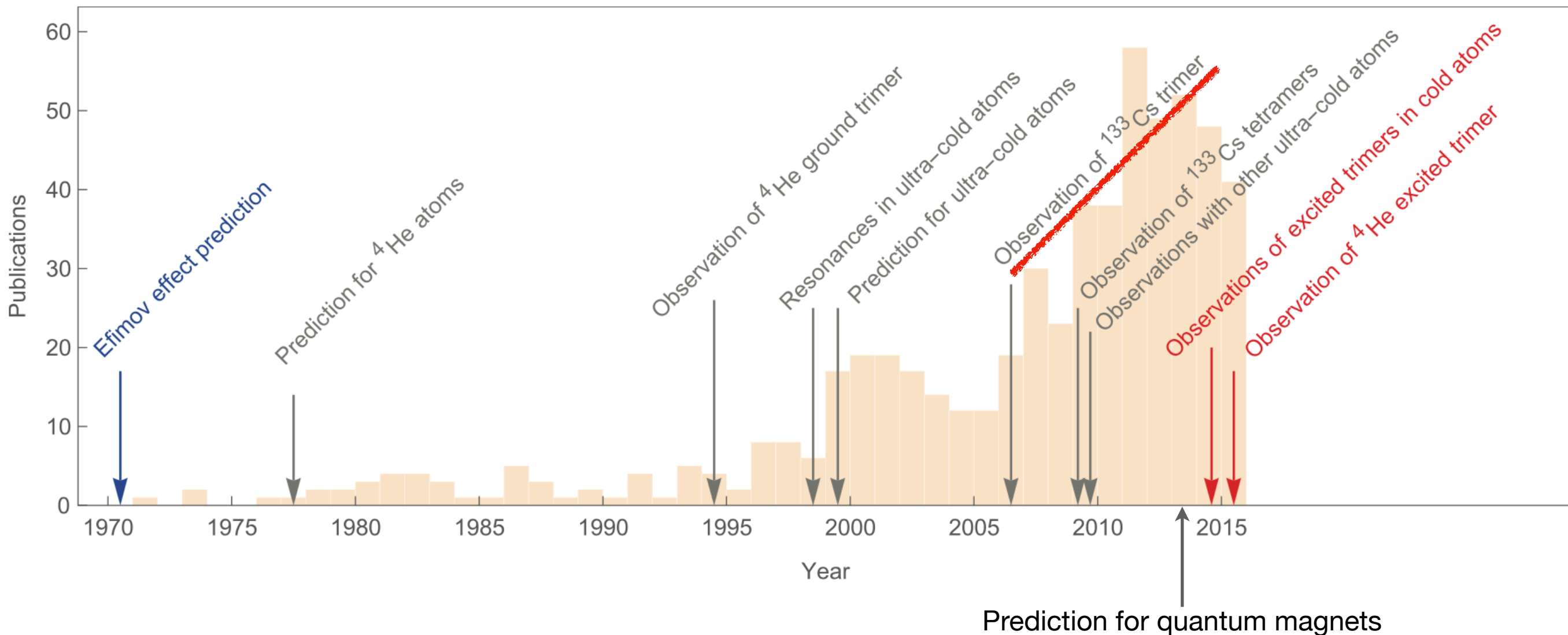
When two bosons interact with $a = \pm \infty$, three bosons form an **infinite** tower of three-body bound states in 3D.

Discrete scale invariance



Efimov effect

P. Naidon & S. Endo, *Rep. Prog. Phys.* **80** 056001 (2017)



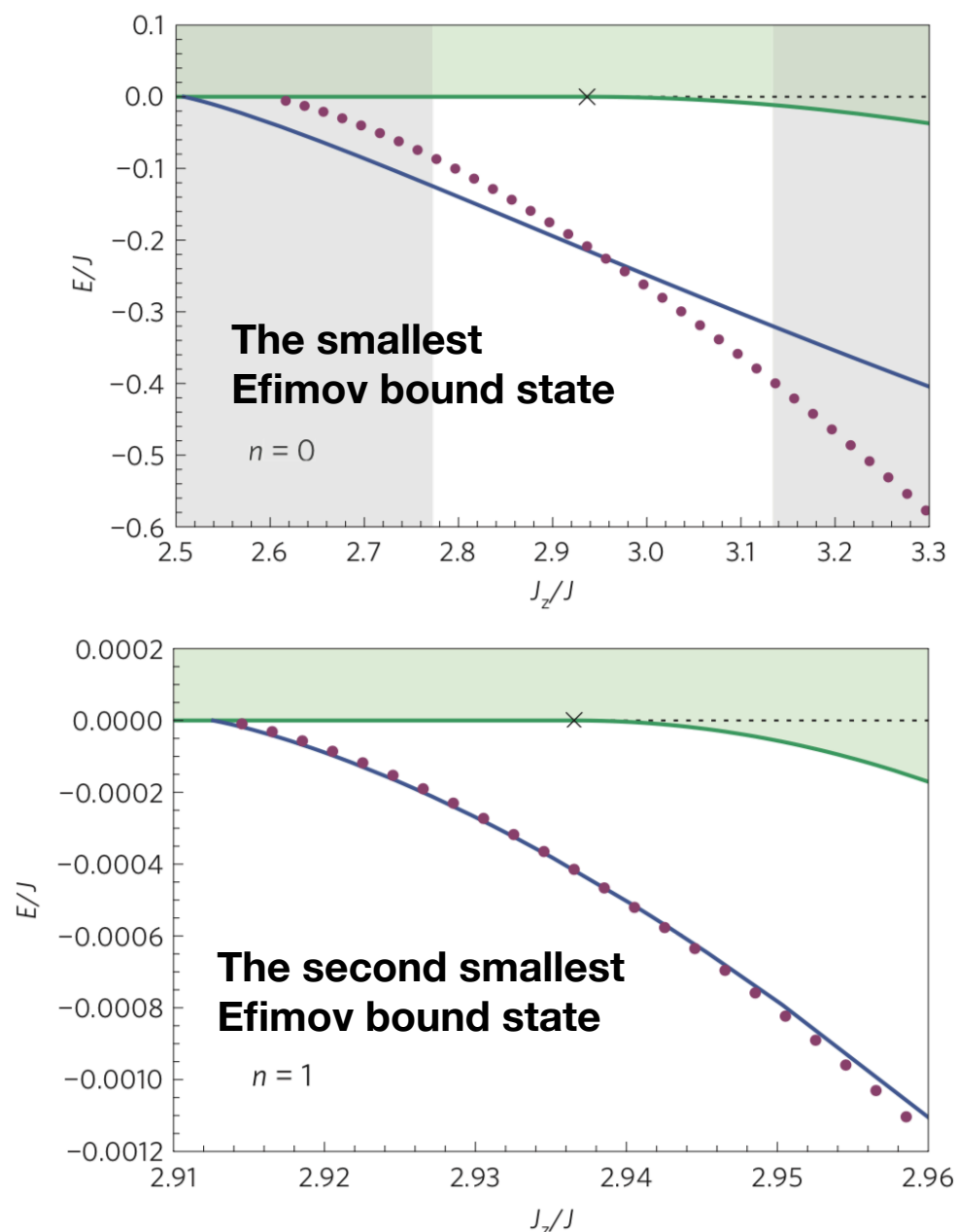
Efimov states have been observed in very limited systems due to the requirement of proximity to a scattering resonance.

Efimov effect in magnets were predicted but has not been observed yet.

Efimov effect in quantum magnets

Y. Nishida, Y.K. & C.D. Batista, Nat. Phys. 9, 93 (2013).

$S = 1/2$ and $S = 1$ XXZ model and $S = 1$ Heisenberg model with uniaxial anisotropy on a simple cubic lattice

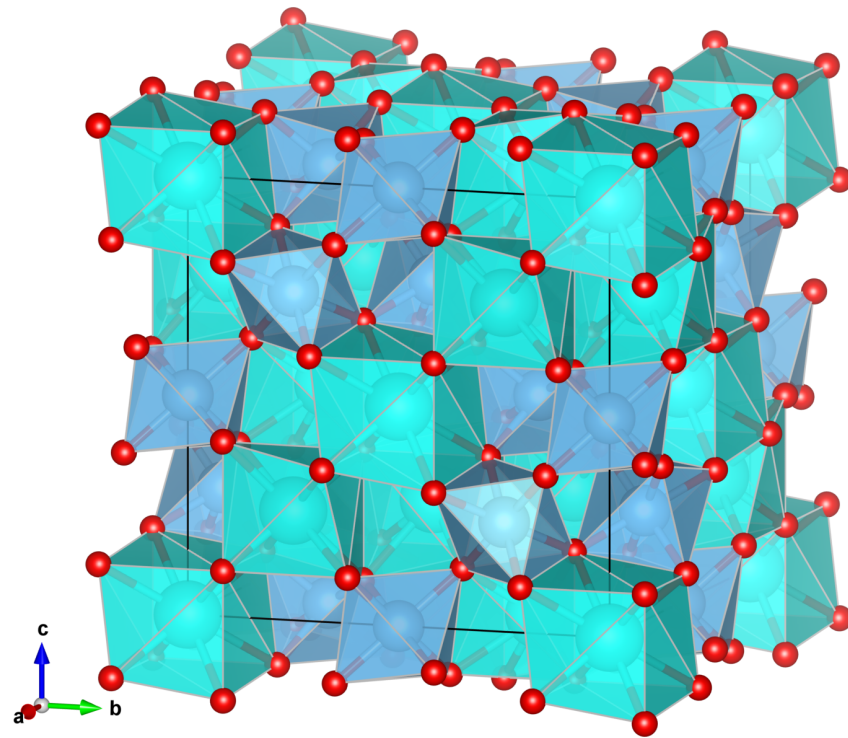


Two lowest binding energies of three magnons for $S = 1/2$ near the two-magnon resonance.

Table 1 Few lowest binding energies of three magnons right at the two-magnon resonances.					
S	J_z/J	D/J	n	E_n/J	$\sqrt{E_{n-1}/E_n}$
1/2	2.93654	—	0	-2.09×10^{-1}	—
			1	-4.15×10^{-4}	22.4
			2	-8.08×10^{-7}	22.7
1	4.87307	0	0	-5.16×10^{-1}	—
			1	-1.02×10^{-3}	22.4
			2	-2.00×10^{-6}	22.7
1	+1	4.76874	0	-5.50×10^{-2}	—
			1	-1.16×10^{-4}	21.8
			2	-2.00×10^{-6}	22.7
1	-1	5.12703	0	-4.36×10^{-3}	—
			1	-8.88×10^{-6}	22.2
—	—	—	∞	—	22.6944

Universal ratio $\lambda \sim 22.7$ is confirmed.
Efimov effect in quantum magnets is predicted.

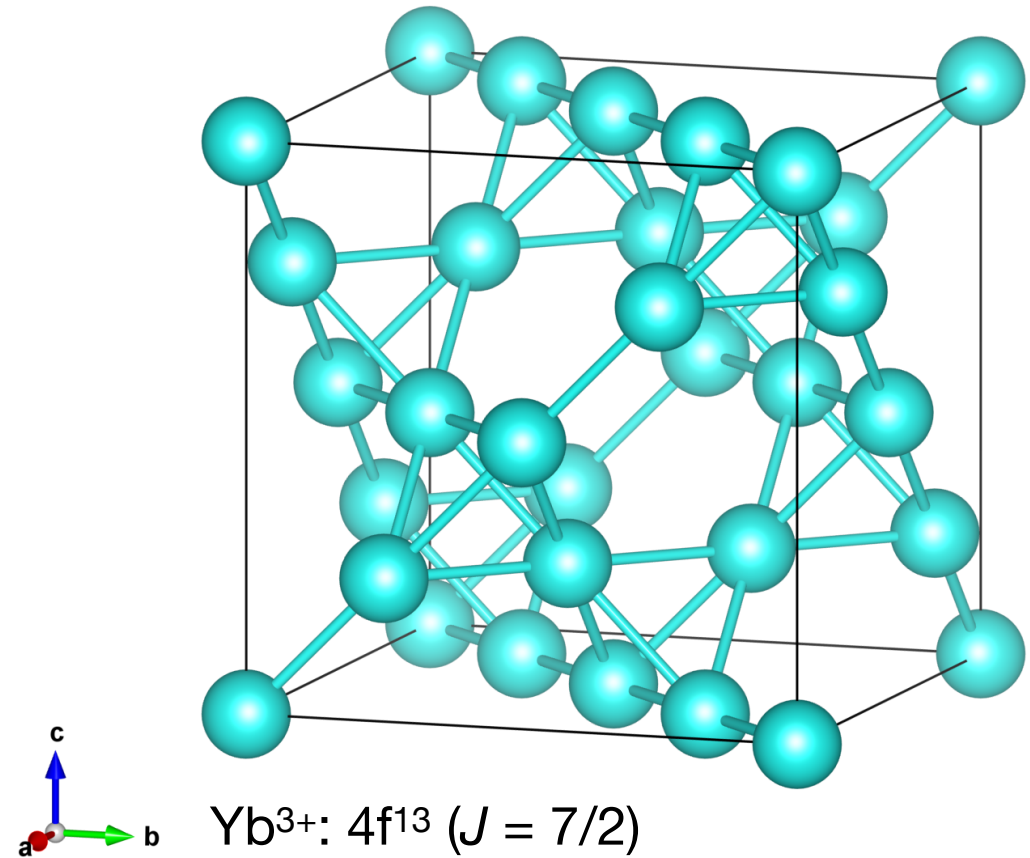
Candidate material: $\text{Yb}_2\text{Ti}_2\text{O}_7$



H. Blöte et al., Physica **43**, 549 (1969)

A.V. Shlyakhtina et al., Solid State Ionics **179**, 1004 (2008)

Yb^{3+} ions form a pyrochlore lattice.



Yb^{3+} : $4f^{13}$ ($J = 7/2$)

Spin orbit coupling & crystalline electric field
→ GS Kramers doublet:= spin-1/2

Detailed analysis: J. Gaudet et al., PRB **92**, 134420 (2015)

Focused material $\text{Yb}_2\text{Ti}_2\text{O}_7$

- ferromagnetically ordered at 270 mK
- competition between ferromagnetism and antiferromagnetism
- magnetic ground state remains a matter of debate at zero field

Model and methods

Model

● Spin Hamiltonian (four-sublattice)

↓ exact mapping

● Hard-core boson model

↓ perturbation theory

● Effective boson model (two-sublattice) (★ number conserved)

spin-1/2 degree of freedom on Yb³⁺

$$\begin{aligned} \mathcal{H}_{\text{spin}} = \sum_{\langle \mathbf{r}\mathbf{r}' \rangle} [& J_{zz} S_{\mathbf{r}}^z S_{\mathbf{r}'}^z - J_{\pm} (S_{\mathbf{r}}^+ S_{\mathbf{r}'}^- + \text{h.c.}) \\ & + J_{\pm\pm} (\gamma_{\alpha_{\mathbf{r}}\alpha_{\mathbf{r}'}} S_{\mathbf{r}}^+ S_{\mathbf{r}'}^+ + \text{h.c.}) \\ & + J_{z\pm} \{ S_{\mathbf{r}}^z (\zeta_{\alpha_{\mathbf{r}}\alpha_{\mathbf{r}'}} S_{\mathbf{r}'}^+ + \text{h.c.}) + (\mathbf{r} \leftrightarrow \mathbf{r}') \}] \\ & - \mu_B \mu_0 H^\mu \sum_{\mathbf{r}} g_{\alpha_{\mathbf{r}}}^{\mu\nu} S_{\mathbf{r}}^\nu. \end{aligned} \quad \mathbf{H} \parallel [110]$$

Methods

● Exact diagonalization

● Lippmann-Schwinger equation

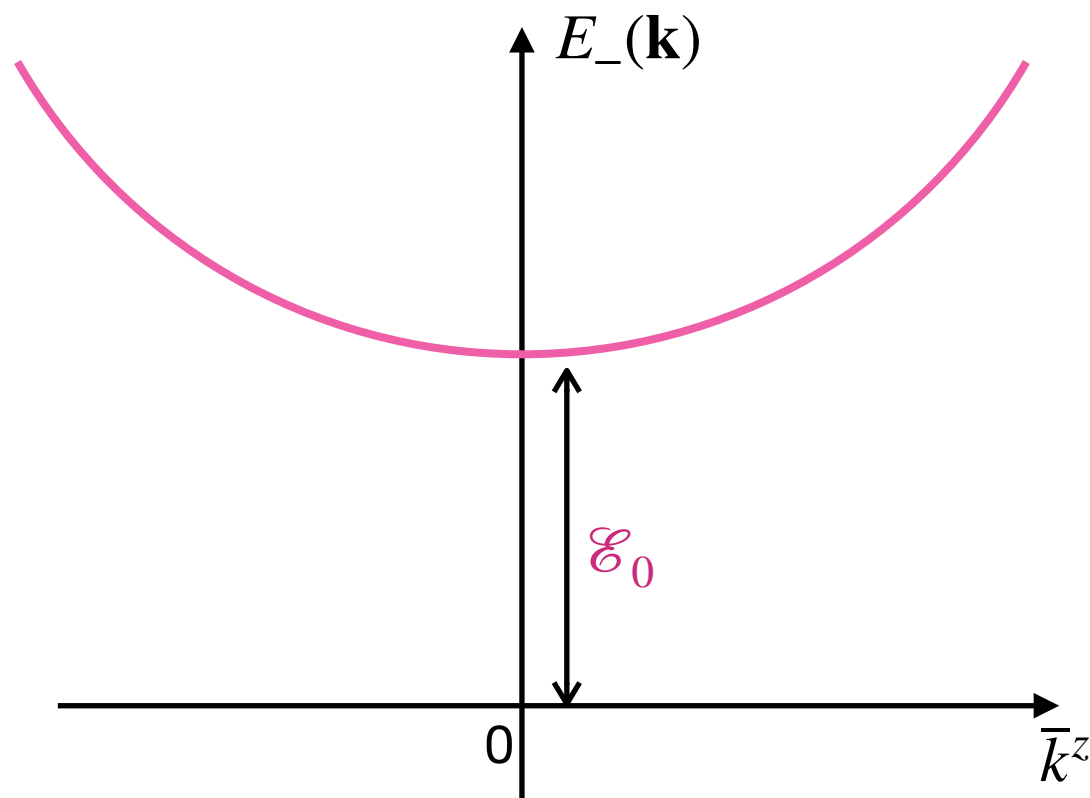
Parameter sets determined by the inelastic neutron scattering experiment [e.g., J.D. Thompson *et al.*, PRL 2017].

$$\begin{aligned} J_{zz} &= 0.026(3) \text{ meV}, & J_{\pm\pm} &= 0.048(2) \text{ meV}, \\ J_{\pm} &= 0.074(2) \text{ meV}, & J_{z\pm} &= -0.159(2) \text{ meV}, \\ g_{\parallel} &= 2.14(3), & g_{\perp} &= 4.17(2). \end{aligned}$$

Results

- Single-magnon spectrum
- Two-magnon resonance
- Three-magnon Efimov states

Single-magnon spectrum



Lower branch of the dispersion:

$$E_-(\mathbf{k}) \simeq \mathcal{E}_0 + \frac{\bar{\mathbf{k}}^2}{2m_z} \quad (|\bar{\mathbf{k}}| \ll 1)$$

$\bar{\mathbf{k}}$: Normalized wave vector

$$\begin{cases} m_z^{-1} = 0.0399 \text{ meV} \\ m_x^{-1} = 0.0425 \text{ meV} \end{cases} \text{ at } \mu_0 H = 12.91 \text{ T}$$

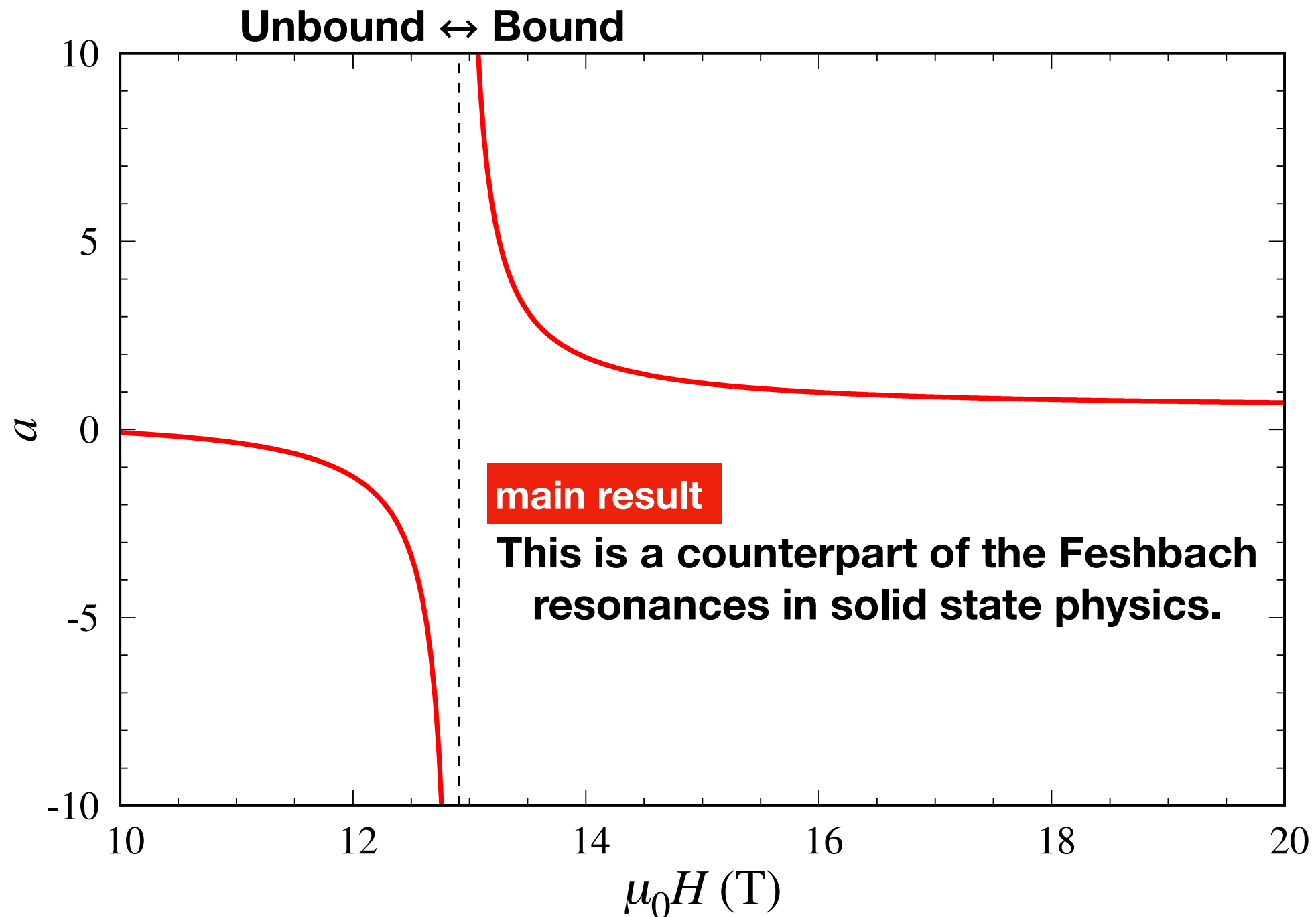
(almost isotropic)

m_z : mass for $\mathbf{k} \parallel [110]$

m_x : mass for $\mathbf{k} \perp [110]$

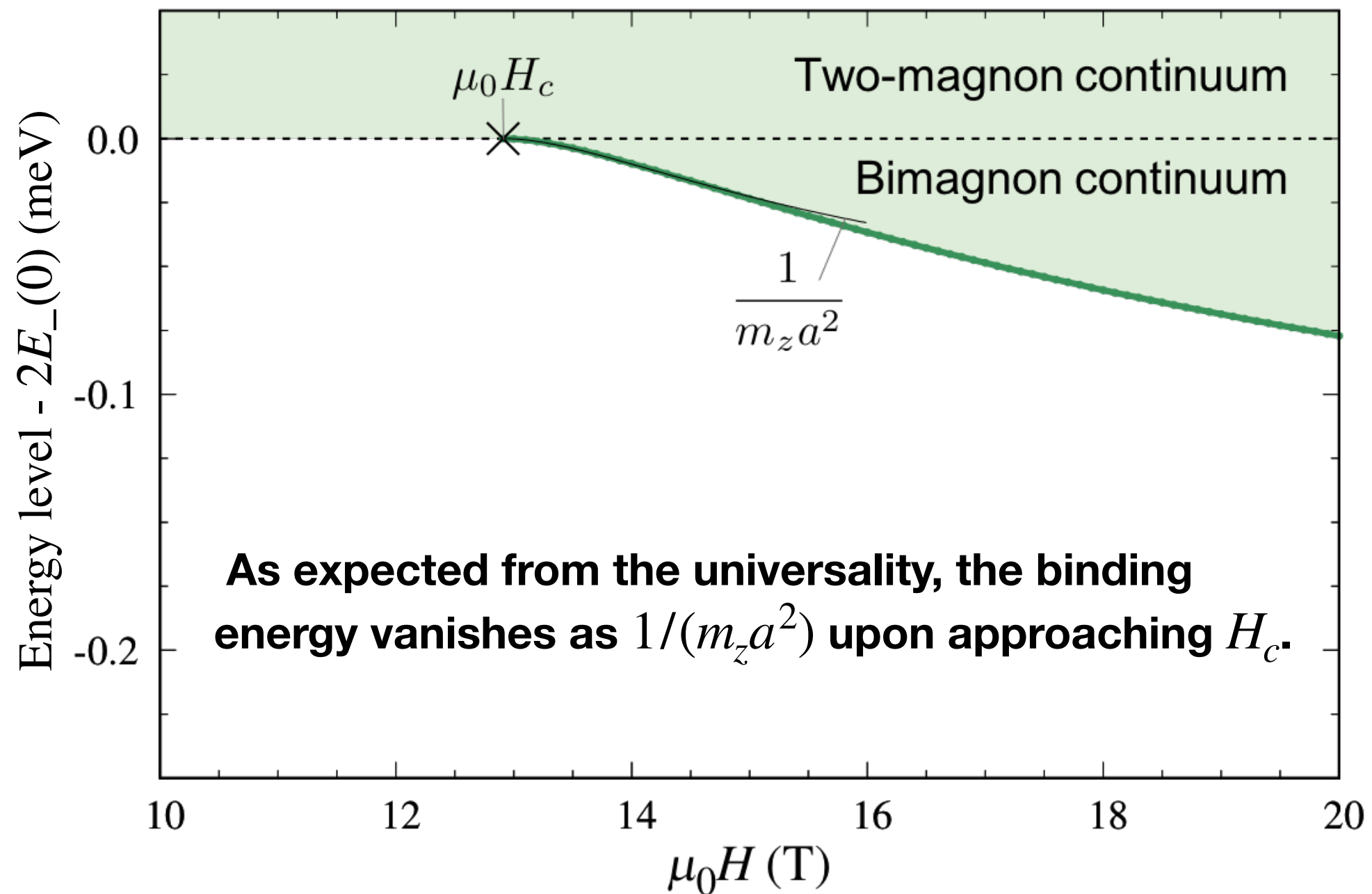
The low-energy physics of $\text{Yb}_2\text{Ti}_2\text{O}_7$ is described by bosons in continuous space with the anisotropic mass tensor.

Two-magnon resonance



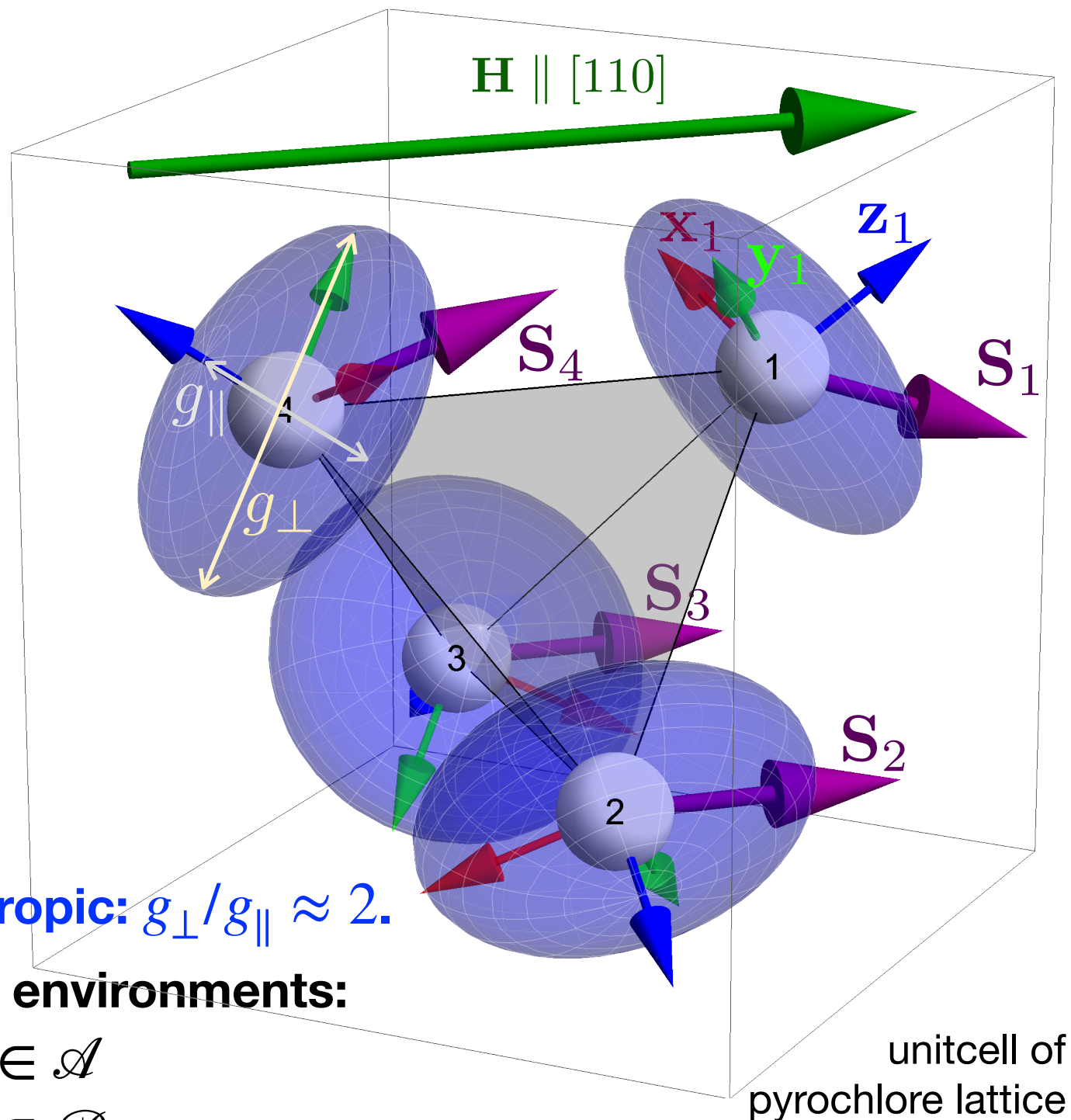
The s-wave scattering length is expected to diverge at $\mu_0 H_c = 12.91$ T.

Two-magnon resonance



Mechanism (1/3)

Spin orientation in large $\mathbf{H} \parallel [110]$ limit

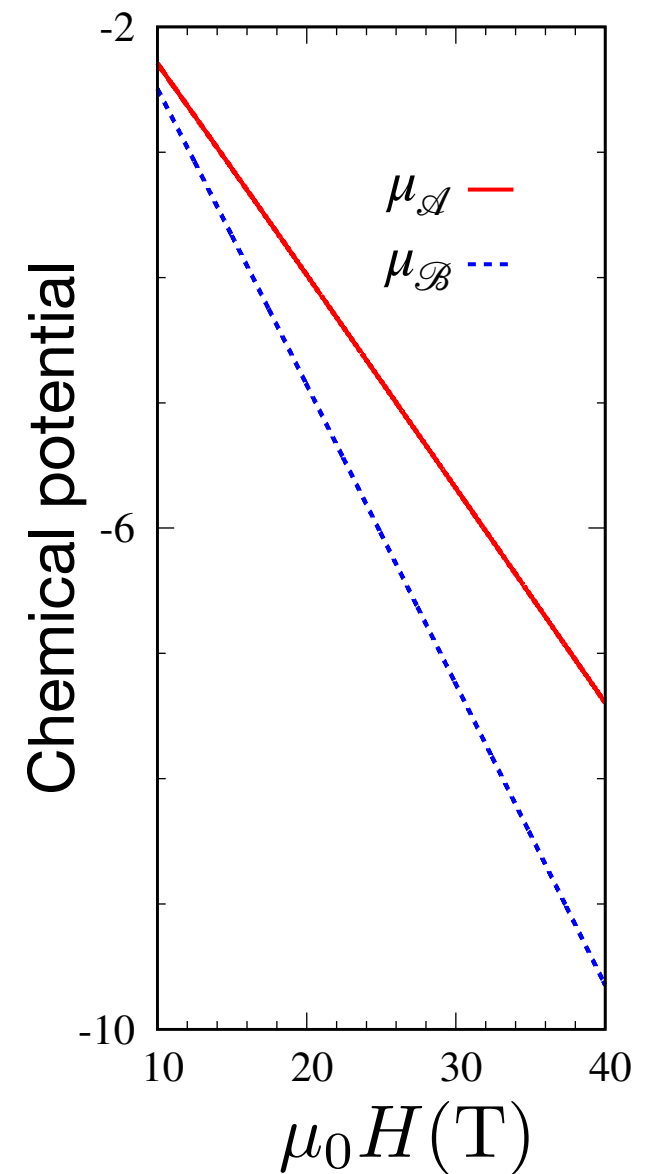


\mathbf{g} -tensor is anisotropic: $g_{\perp}/g_{\parallel} \approx 2$.

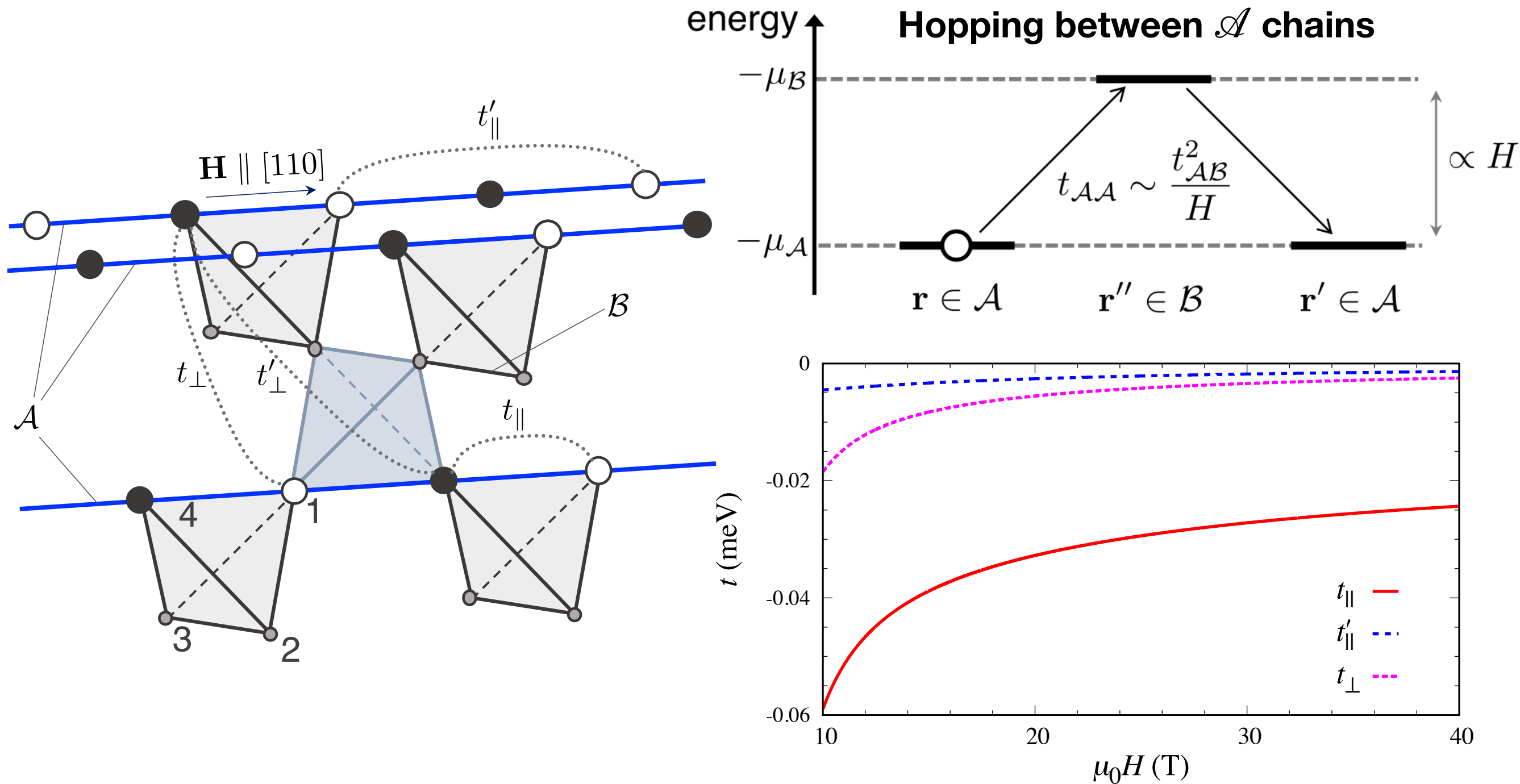
Two different local environments:

sublattice 1 and 4 $\in \mathcal{A}$

sublattice 2 and 3 $\in \mathcal{B}$



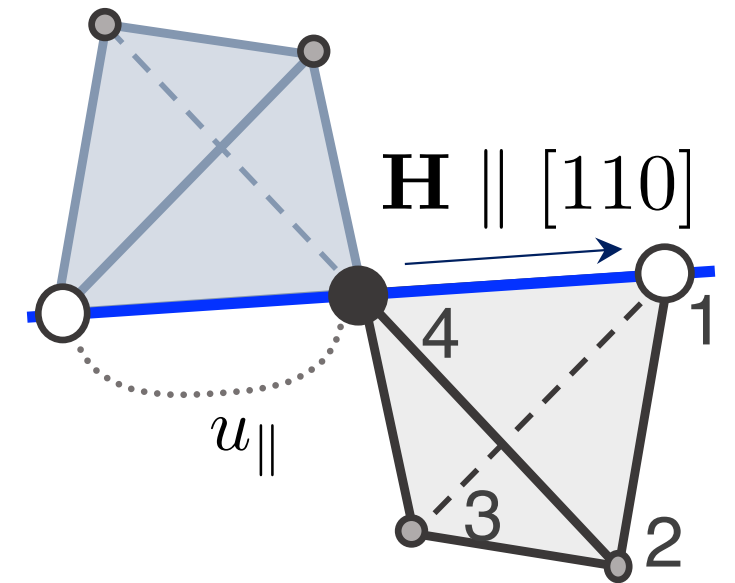
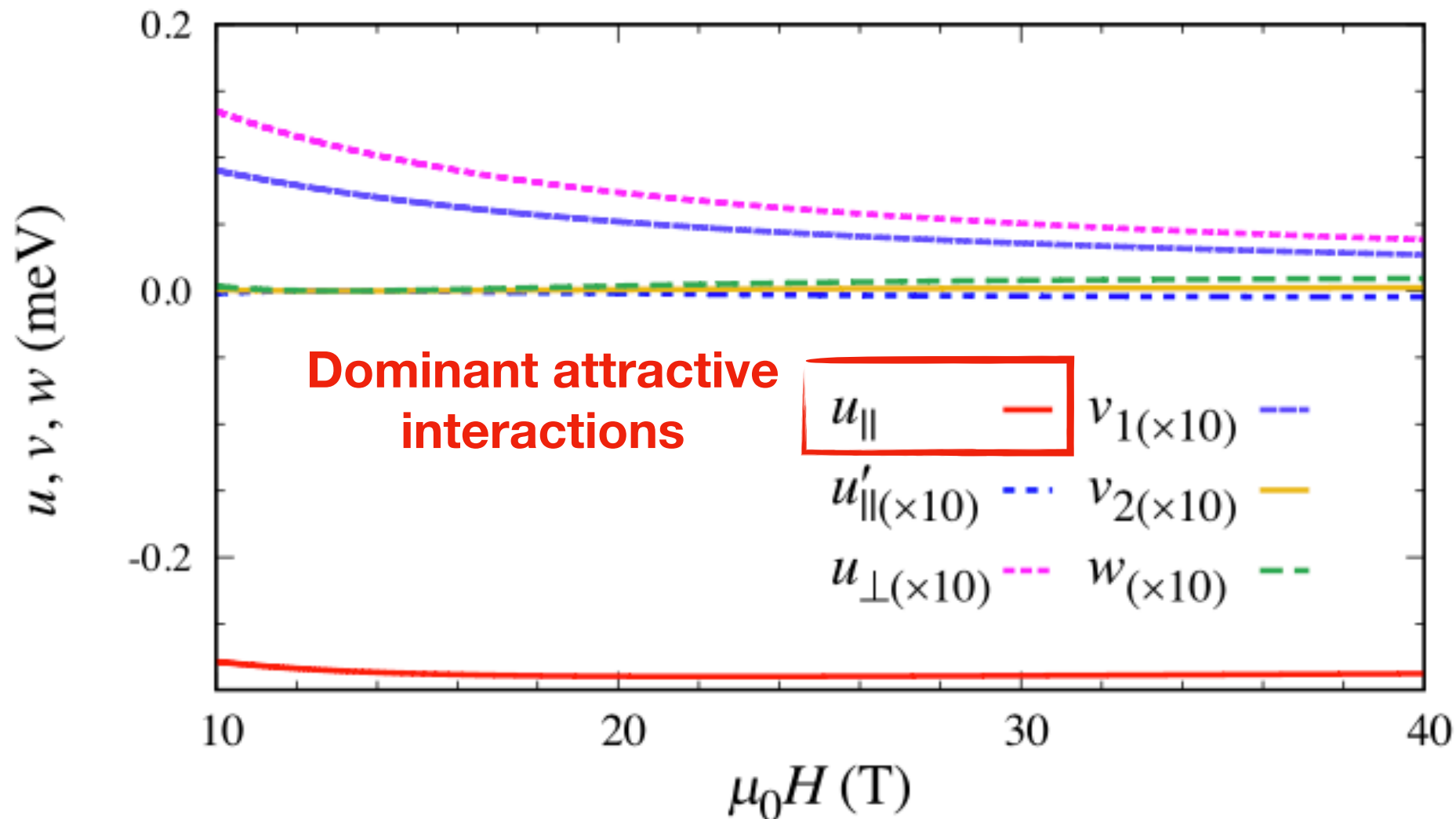
Mechanism (2/3)



A part of kinetic energy is suppressed by an external magnetic field.

Mechanism (3/3)

Attractive interaction is insensitive to the external magnetic field.



Dominant attractive interaction in large $\mathbf{H} \parallel [110]$ limit:

$$u_{\parallel} \approx \frac{2}{2g_{\parallel}^2 + g_{\perp}^2} \left[2\sqrt{2}g_{\parallel}g_{\perp}J_{z\pm} + g_{\perp}^2(J_{\pm} - J_{\pm\pm}) - g_{\parallel}^2J_{zz} \right]$$

The main factor of the large u_{\parallel} is due to the large $-J_{z\pm}$.

$$\begin{aligned}
 J_{zz} &= 0.026(3) \text{ meV}, & J_{\pm\pm} &= 0.048(2) \text{ meV}, \\
 J_{\pm} &= 0.074(2) \text{ meV}, & J_{z\pm} &= -0.159(2) \text{ meV}, \\
 g_{\parallel} &= 2.14(3), & g_{\perp} &= 4.17(2).
 \end{aligned}$$

J.D. Thompson *et al.*, PRL 2017

Two-magnon resonance

- Other parameter sets for $\text{Yb}_2\text{Ti}_2\text{O}_7$

Parameter set	J_1 (meV)	J_2 (meV)	J_3 (meV)	J_4 (meV)	J_{zz} (meV)	J_{\pm} (meV)	$J_{z\pm}$ (meV)	$J_{\pm\pm}$ (meV)	g_{xy}	g_z
Ross (10)	-0.09	-0.22	-0.29	+0.01	0.17	0.05	-0.14	0.05	4.32	1.8
Thompson (3)	-0.028	-0.326	-0.272	+0.049	0.026	0.074	-0.159	0.048	4.17	2.14
Robert (11)	-0.03	-0.32	-0.28	+0.02	0.07	0.085	-0.15	0.04	?	?
This study	-0.026(2)	-0.307(3)	-0.323(3)	+0.028(2)	0.094	0.087	-0.161	0.0611	4.17	2.14

Table S4. Spin Hamiltonian parameter sets used in the paper in two notations for $\text{Yb}_2\text{Ti}_2\text{O}_7$. The reported parameters from one notation were directly converted to the other notation (without accounting for error bars) unless already provided in the reference.

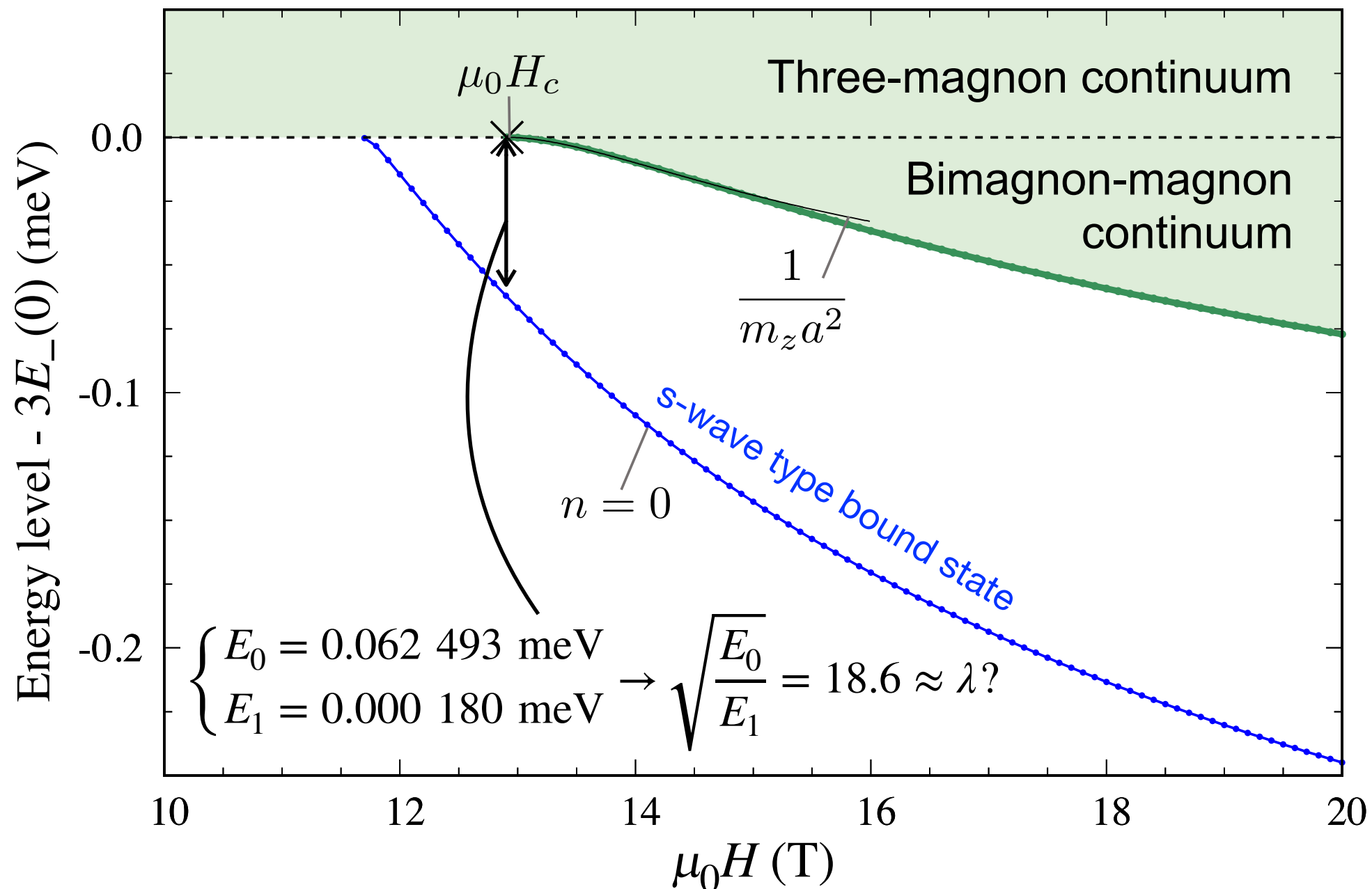
from A. Scheie *et al.*, PNAS **117**, 27245 (2020)

$$\begin{aligned}
 \text{Ross } et al. &\rightarrow \mu_0 H_c = 9.09 \text{ (T)} \\
 \text{Joubert } et al., \& \text{ Bowman } et al. &\rightarrow \mu_0 H_c = 8.80 \text{ (T)} \\
 \text{Thompson } et al. &\rightarrow \mu_0 H_c = 12.91 \text{ (T)} \\
 \text{Robert } et al. &\rightarrow \mu_0 H_c = 11.81 \text{ (T)} \\
 \text{Scheie } et al. &\rightarrow \mu_0 H_c = 11.48 \text{ (T)}
 \end{aligned}$$

- $\text{Yb}_2\text{Ge}_2\text{O}_7$ [C.L. Sarkis *et al.*, Phys. Rev. B **102**, 134418 (2020)] $\rightarrow \mu_0 H_c = 14.80 \text{ (T)}$

The two-magnon resonance is expected to be realized at experimentally reachable magnetic field.

Three-magnon Efimov states



The s-wave type bound states ($n = 0$ and $n = 1$) are found near the resonance.



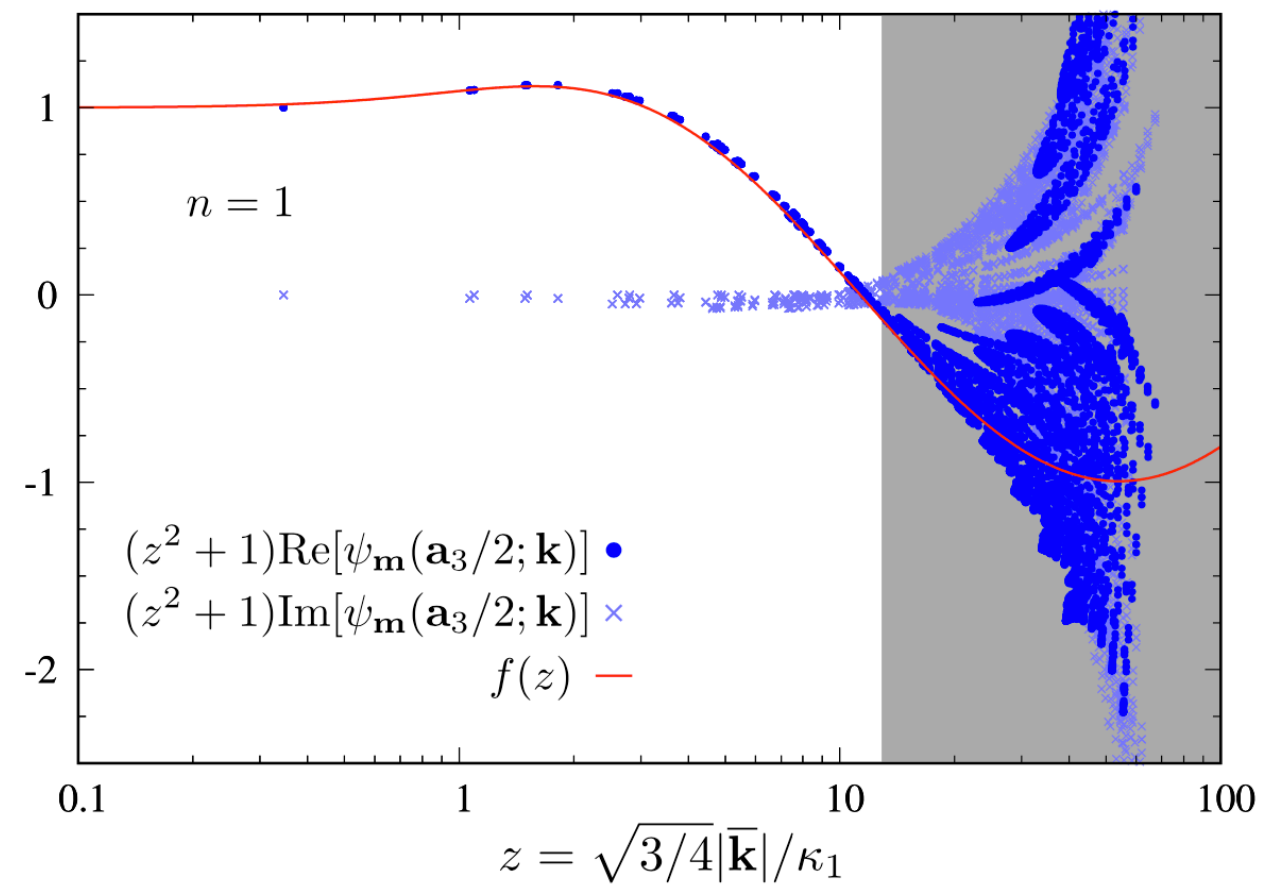
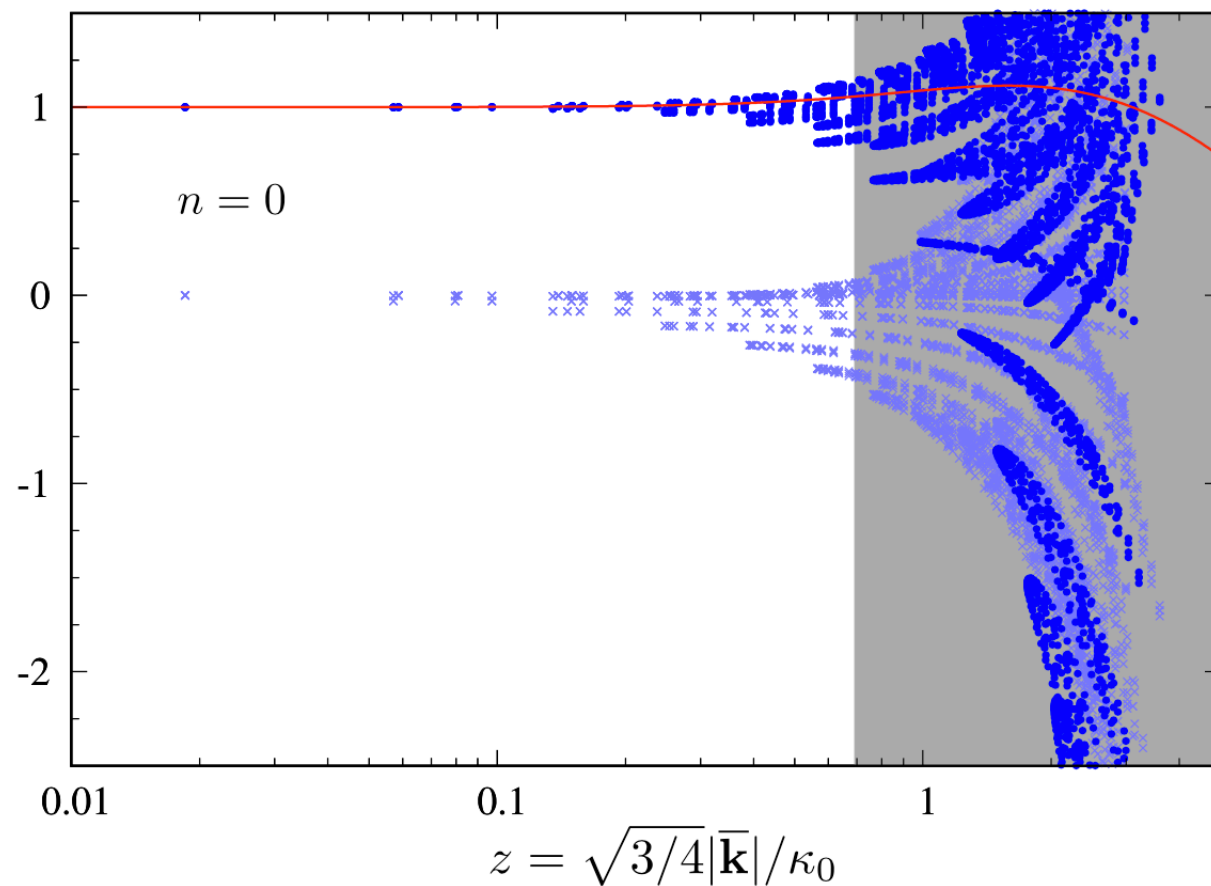
Analysis of the wave functions

Three-magnon Efimov states

Comparison with the universal function $f(z)$ at H_c

$$\kappa_n = \sqrt{m_z E_n}$$

nonuniversal regime
 $|\bar{\mathbf{k}}| > 1$



The excellent agreement in the long wavelength region ($|\mathbf{k}| < 1$)



Although the $n = 0$ state may not, the $n = 1$ state is identified as the Efimov state.

Experimental realization

- Raman scattering is the ideal technique for observing two-magnon bound states [M.F. Thorpe, PRB(1971), B.S. Shastry & B.I. Shraiman, PRL(1990)].

→ The resonance condition can be identified.

- The number non-conserved terms proportional to na^\dagger exit in the hard core boson model before the approximation based on the perturbation theory.

→ Two-magnon states are mixed to the three-magnon bound states as an $\mathcal{O}(J/H)$ perturbation.

→ Three-magnon bound states could be also observed via Raman spectroscopy.

Summary

- The magnetic field acts as a knob to tune the s-wave scattering length of magnons in $\text{Yb}_2\text{Ti}_2\text{O}_7$ (**counterpart of Feshbach resonance**).
- A two-magnon resonance condition is achieved at an experimentally reachable magnetic field strength of $H_c \sim 13$ T along the $[110]$ direction.
- In our calculations, a couple of three-magnon bound states with the s-wave wave function were found just below the three-magnon continuum of the excitation spectrum near H_c .
- While the ground state ($n = 0$) exhibits some deviations from the universal character due to lattice effects, the first excited state ($n = 1$) is indeed an Efimov state.

Publication:

Y. Kato, S.-S. Zhang, Y. Nishida, and C.D. Batista, Phys. Rev. Research **2**, 033024 (2020).